Monthly Notices
of the
ROYAL ASTRONOMICAL SOCIETY

MNRAS **457,** 496–509 (2016) doi:10.1093/mnras/stv2971

A simple way to improve AGN feedback prescription in SPH simulations

Kastytis Zubovas,[1]★ Martin A. Bourne[2,3] and Sergei Nayakshin[2]

[1] *Center for Physical Sciences and Technology, Savanorių 231, Vilnius LT-02300, Lithuania*
[2] *Department of Physics & Astronomy, University of Leicester, Leicester LE1 7RH, UK*
[3] *Institute of Astronomy and Kavli Institute for Cosmology, University of Cambridge, Madingley Road, Cambridge CB3 0HA, UK*

Accepted 2015 December 17. Received 2015 December 17; in original form 2015 July 17

ABSTRACT

Active galactic nuclei (AGN) feedback is an important ingredient in galaxy evolution, however its treatment in numerical simulations is necessarily approximate, requiring subgrid prescriptions due to the dynamical range involved in the calculations. We present a suite of smoothed particle hydrodynamics simulations designed to showcase the importance of the choice of a particular subgrid prescription for AGN feedback. We concentrate on two approaches to treating wide-angle AGN outflows: thermal feedback, where thermal and kinetic energy is injected into the gas surrounding the supermassive black hole (SMBH) particle, and virtual particle feedback, where energy is carried by tracer particles radially away from the AGN. We show that the latter model produces a far more complex structure around the SMBH, which we argue is a more physically correct outcome. We suggest a simple improvement to the thermal feedback model – injecting the energy into a cone, rather than spherically symmetrically – and show that this markedly improves the agreement between the two prescriptions, without requiring any noticeable increase in the computational cost of the simulation.

Key words: accretion, accretion discs – methods: numerical – ISM: evolution – quasars: general.

1 INTRODUCTION

Feedback from active galactic nuclei (AGN) is a key ingredient in modern galaxy evolution models. It is required in order to explain the sharp drop-off in the galaxy mass function above $M_* \simeq 10^{11}\,\mathrm{M}_\odot$, prevent the cooling catastrophe in galaxy clusters and produce the hot gas atmospheres seen around many galaxies. Observations of massive kpc-scale outflows (Feruglio et al. 2010; Rupke & Veilleux 2011; Sturm et al. 2011; Cicone et al. 2014) and pc-scale relativistic winds (Tombesi et al. 2010a,b) provide further evidence that AGN affect their host galaxies in a significant way.

One outstanding issue in understanding the precise effects of feedback is the range of spatial scales over which it operates. The AGN jets and winds are launched from the accretion disc on scales $l_{\rm min} < 0.01$ pc, while the observed effects on host galaxies span 10^3 pc or more. This means that in order to model the AGN feedback precisely, a simulation should span at least five orders of magnitude in linear scale, resulting in 10^{15} resolution elements for a 3D model, a resolution which is not likely to be reached any time soon. Even resolving the interaction of an AGN wind with the host galaxy material, on scales of several parsecs and larger, is currently only possible in single-galaxy models, rather than cosmological simulations (Schaye et al. 2015).

As a result of this shortcoming, some effects of AGN feedback might not be apparent from simulations. In a recent paper (Bourne, Zubovas & Nayakshin 2015), we showed that mass resolution has a significant influence upon the AGN feedback effects seen in simulations of turbulent gas. In particular, at mass resolutions typical of cosmological simulations, we found AGN feedback to be much more negative, in the sense of efficiency of gas removal, than at higher resolution. In high-resolution simulations, AGN winds expel only diffuse gas, while denser gas forms filaments which fall in towards the central supermassive black hole (SMBH) and can potentially feed it or form stars. These results suggest that AGN feedback can be positive as well as negative, increasing the star formation rate (SFR) in its host. Our other previous research (Nayakshin & Zubovas 2012; Zubovas et al. 2013; Bourne, Nayakshin & Hobbs 2014) provides some support for this conclusion as well. Several other authors have investigated similar positive AGN feedback coming from the interaction of the jet with the galactic ISM (Silk 2005; Gaibler et al. 2012).

In this paper, we investigate another numerical aspect of modelling AGN feedback: the prescription detailing how the AGN feedback energy is passed to the surrounding gas. We perform high-resolution simulations of AGN feedback acting upon a turbulent gas reservoir, passing the feedback energy in one of two ways: a Monte Carlo radiative transfer scheme, which self-consistently takes into account gas optical depth; and a kernel-weighted thermal and kinetic energy input scheme. We find that the Monte Carlo

★ E-mail: kastytis.zubovas@ftmc.lt

© 2016 The Authors
Published by Oxford University Press on behalf of the Royal Astronomical Society

scheme, while being numerically far more expensive and difficult to scale, provides qualitatively different results than thermal and kinetic energy injection. In particular, the Monte Carlo scheme allows the formation of simultaneous gas inflows and outflows, resulting in prolonged AGN feeding and faster, but less massive, outflows. We also test an adjusted version of both schemes, where the feedback energy is injected, or virtual particles released, biconically, rather than spherically symmetrically. This change makes the results of the two schemes significantly more alike. We suggest that using this improvement to the thermal feedback prescriptions would make the results of large-scale numerical simulations much more realistic.

The structure of the paper is as follows. In Section 2, we describe the numerical model and setup used in the simulations. The simulation results are presented in Section 3. We discuss the implications of our work for both numerical modelling of galaxy evolution and interpretation of observations in Section 4 and conclude in Section 5.

2 NUMERICAL MODEL

2.1 Basics of the model

The code used is GADGET-3, an updated version of the publicly available GADGET-2 (Springel 2005). It is a hybrid *N*-body/SPH code with individual particle timesteps and adaptive smoothing. We employ the SPHS extension of the basic smoothed particle hydrodynamics (SPH) scheme (Read & Hayfield 2012), which improves the modelling of mixing within a multiphase medium, allowing us to better track the interaction between turbulent gas flows. We use a Wendland kernel (Wendland 1995; Dehnen & Aly 2012) with 100 neighbours.

The initial conditions of all models presented in this paper are the same. They consist of a gas sphere with isothermal density profile, extending from $R_{\rm in} = 100$ pc to $R_{\rm out} = 1$ kpc. The gas sphere is resolved with 10^6 particles, giving a particle mass of $m_{\rm SPH} = 3000\,{\rm M}_\odot$ and a mass resolution of $m_{\rm res} = 100\,m_{\rm SPH} = 3\times10^5\,{\rm M}_\odot$. The spatial resolution of the model varies depending on gas density, but is generally of the order a few pc; we adopt a minimum gravitational and SPH smoothing length of 0.1 pc. The gas is embedded in a static isothermal background density profile with velocity dispersion $\sigma = 200\,{\rm km\,s^{-1}}$, and is supported against the background gravity by turbulent motion with characteristic velocity $v_{\rm turb} = \sigma$. The gas is initially cold ($c_{\rm s} \ll v_{\rm turb}$; see below for a discussion on how the gas evolves thermally). An SMBH is embedded in the centre of the gas distribution and can swallow gas which comes within the accretion radius $r_{\rm accr} = 10$ pc of the SMBH particle and is energetically bound to it. We set the SMBH particle mass to $2\times10^8\ {\rm M}_\odot$, in order for the radius of its sphere of influence to be $r_{\rm infl} \simeq r_{\rm accr}$. This ensures that the gas moves in a purely isothermal background potential only perturbed by its own self-gravity, rather than the gravity of the SMBH. The SMBH is inactive for the first 1 Myr of the simulation; this allows the gas to develop a turbulent density structure before it is affected by feedback. In order to prevent the formation of spurious high-density filaments close to the inactive SMBH, we extend the accretion radius to $r'_{\rm accr} = R_{\rm in}$ during this time. After 1 Myr, the AGN switches on for 1 Myr and begins affecting the gas in two ways.

First of all, we model the effect of the AGN radiation field by employing a Sazonov et al. (2005) cooling curve, appropriate for optically thin gas subjected to AGN radiation. Below $T = 10^4$ K, we extend the cooling curve with the one proposed by Mashchenko, Wadsley & Couchman (2008) down to a temperature floor, which depends on the gas density such that the Jeans mass of the gas never falls below the resolution limit.

Gas particles which fall on this dynamic temperature floor are stochastically converted into sink particles in order to speed up the simulations. This is equivalent to having a density threshold

$$\rho_{\rm J} = \left(\frac{\pi k_{\rm B} T}{\mu m_{\rm p} G}\right)^3 m_{\rm res}^{-2} \simeq 6.7\times10^{-15} T_4^3\ {\rm g\,cm^{-3}}, \quad (1)$$

$$n_{\rm J} \simeq 6.2\times10^9 T_4^3\ {\rm cm^{-3}}, \quad (2)$$

where $T_4 \equiv T/10^4$ K. This crude approximation of the star formation process may affect our results slightly, because sink particles are affected only by gravity and cease to interact with the AGN feedback. Since sink particles are created in dense gas, this slightly reduces the fraction of feedback energy received by dense gas and increases the fraction received by diffuse gas. On the other hand, we do not model the effects of self-shielding of dense gas clumps, so the reduction in received energy caused by the formation of sink particles mimics that effect to some extent. In any case, this effect is small, since our simulations never produce more than 10^4 sink particles.

The other way that the AGN affects the gas is by means of wind feedback, which we describe below.

2.2 Physics and implementation of AGN feedback

The AGN wind feedback model (King 2003, 2010) has a number of appealing properties: it is based upon relatively well-understood physical processes; it can explain the M–σ relation without requiring free parameters; it can explain the properties of observed fast AGN winds on sub-parsec scales, as well as those of massive AGN outflows on kpc scales (Zubovas & King 2012). Observations show that winds with velocity $v_{\rm w} \sim 0.1\,c$ and power $L_{\rm kin} \sim 0.05 L_{\rm AGN}$ are present in a large fraction of AGN (Tombesi et al. 2010a,b), suggesting a wide opening angle (Nardini et al. 2015). In the wind feedback model, these winds shock against the galactic ISM and drive large-scale outflows (King 2010). The shocked wind passes its energy and momentum to the ISM, accelerating the outflow to $v_{\rm out} > 1000\,{\rm km\,s^{-1}}$ (Zubovas & King 2012). However, a large fraction of the outflow energy can leak out through gaps in the non-uniform ISM, leading to a situation where some of the gas is outflowing with large velocities, while dense gas is simultaneously inflowing towards the SMBH (Nayakshin 2014; Zubovas & Nayakshin 2014).

Therefore, it is important to check how well numerical simulations can capture this complex process of simultaneous inflow and outflow on scales from tens to thousands of parsecs. We do this by exploring two subgrid feedback implementations and their improvements.

2.2.1 *Thermal feedback model*

The simplest feedback prescription, often used in cosmological models, is the 'thermal feedback' subgrid prescription. In this prescription, the feedback energy of the AGN, which we take to be $\epsilon_{\rm f} = 5$ per cent of its luminous energy output over the SMBH timestep, is passed as thermal energy to the SMBH particle neighbours. We choose 100 neighbours for the SMBH particle, the same as for gas particle. Testing showed that using fewer neighbours results in feedback becoming extremely inefficient, as gas particles can be accreted by the SMBH even after being heated; however, if

the particles were not accreted, it is likely that the feedback would be more efficient as the temperature would be higher and so the cooling time would increase. Meanwhile, using more neighbours dilutes the feedback and results in faster cooling of gas (Bourne et al. 2015).

The feedback energy given to each particle is weighted by the SPH interpolation kernel. This means that gas closer to the SMBH receives proportionately more energy than gas further away.

In addition to thermal energy, each SPH particle receives a similarly kernel-weighted fraction of the AGN wind momentum, $L_{\rm AGN}\,{\rm d}t/c$, in a direction radially away from the SMBH. While this is not usually done in cosmological models, we implement this aspect of feedback in order to be able to do a more direct comparison with the Monte Carlo radiative transfer method. Tests showed that the effect of momentum feedback is negligible compared with the thermal energy input.

2.2.2 *Biconical thermal feedback model*

One issue with the simple thermal feedback prescription is that the feedback energy is given to the nearest particles without taking their spatial distribution into account. This implicitly assumes that the gas distribution is (approximately) spherically symmetric. A real galaxy contains multiphase gas, with many structures degrading the spherical symmetry, even if such symmetry might be expected on large scales. For the AGN, this results in neighbouring gas particles having very different density and correspondingly very different effective cross-sections. In principle, feedback affecting each particle should be attenuated by calculating the optical depth between the SMBH and this particle. However, doing so is a very time-consuming process, unfeasible to implement in cosmological simulations, which may have many AGN at the same time.

Therefore, we propose a simpler method, which we believe captures some of the important physics. The method relies on injecting the thermal and kinetic energy in a cone centred on the SMBH instead of spherically symmetrically. Spherical symmetry is unlikely on the subgrid scales on which the wind is launched, since the AGN has a preferred plane – that of the accretion disc – and winds are likely to be launched perpendicular to it. So we would expect the wind to be launched with an axisymmetric geometry. This prescription ensures that gas in all direction does not experience identical feedback. Instead, there is a preferred plane for the gas to accrete in, corresponding to the plane of the subgrid accretion disc.

Numerically, we implement this model by calculating a separate neighbour list for the SMBH particle, looking for neighbours only in a bicone with a specified opening angle, which is set to 45 deg in the simulations presented in this paper. For simplicity, we choose the axis of the cone to lie in the Z direction. The number of neighbours in the cone is the same as the number of neighbours used for the hydrodynamics calculations, and the feedback energy input is weighted by the value of the SPH interpolation kernel, only using the larger smoothing length corresponding to the neighbours in the cone.

2.2.3 *Virtual particle model*

The 'virtual particle' Monte Carlo radiative transfer method (Nayakshin, Wilkinson & King 2009) relies on packets of feedback energy, which are emitted by the AGN as particles and move in straight lines with a constant velocity, carrying momentum and energy. When the virtual particle moves into an SPH particle's smoothing kernel, it starts giving up its momentum and energy over several timesteps, distributing it proportionately among all SPH particles which contain the virtual particle in their smoothing kernels. Since the virtual particles are emitted isotropically, the energy injection is also isotropic, independent of the distribution of gas around the SMBH. This ensures that, for example, a dense and small gas clump close to the SMBH does not receive too much of the feedback energy, because the prescription self-consistently takes into account the cross-section of the clump. It also means that even gas very far away from the SMBH may receive a direct energy and momentum input, if the intervening space is empty, for example having been cleared by a progressing outflow.

We test two versions of the virtual particle model: one with spherically symmetric emission of tracer particles, and one where the particles are emitted in a cone with a 45 deg opening angle.

2.3 Model parameters

We present the results of 13 models; their identification labels and main parameters are given in Table 1. One simulation, NoAGN, is intended as a control and does not have any AGN feedback (the SMBH is still present and accretes gas). Then four sets of three models each investigate the effects of different subgrid feedback prescriptions on feedback from AGN of different luminosities. We choose $L_{\rm AGN}$ to span a range of observed quasar luminosities; furthermore, these luminosities encompass the critical luminosity necessary to drive away gas from the AGN by purely momentum feedback (King 2010). The opening angle of the cone in the thermal conical (tkc) and virtual particle conical (vpc) simulations is 45 deg.

3 RESULTS

At first, we briefly discuss the properties of the gas distribution just before the AGN switches on. Then we present the morphology of the spherically symmetric feedback models, vp and tk, and finally move on to their conical feedback counterparts, vpc and tkc. Later, we discuss the resulting gas morphology, outflow energetics, inflow and outflow rates and the density structure.

3.1 Initial evolution of the gas shell

During the first 1 Myr of evolution, the gas shell develops a turbulent density structure and cools down to temperatures in the range 10–10^4 K. Fig. 1 shows the phase diagram of the gas just before the AGN switches on. Most of the gas has temperatures just below 10^4 K, where there is a minimum in the cooling rate. Some gas is located on the temperature floor (diagonal line in the bottom right of the distribution), however the probabilistic conversion of gas into sink particles ensures that only ∼2000 particles have been converted into stars. Approximately 15 per cent, i.e. $4.5 \times 10^8\,{\rm M}_\odot$, of the initial shell has been accreted by the SMBH particle. This makes the SMBH mass grow to more than three times its initial mass, however this does not affect the subsequent results, since we fix the AGN luminosity, rather than tying it to the SMBH mass. It is important to note that during this phase, the accretion radius is set to 100 pc, and most of the gas accreted through this radius is unlikely to reach the SMBH during the time period simulated in our models.

Table 1. Parameters of the numerical models and most important results. The first column shows the model ID. The next two columns give the parameters: the type of AGN feedback prescription used and the AGN luminosity $L_{\rm AGN}$ in units of Eddington luminosity of a $10^8\,{\rm M}_\odot$ SMBH. Then four columns give the primary results at $t = 0.5$ Myr after the AGN switches on: the size of the feedback bubble in kpc, the ratio between gas energy and input energy from the AGN, the mass accretion rate by the SMBH particle, and the mass outflow rate.

Model ID	Feedback model	$\frac{L_{\rm AGN}}{1.3\times10^{46}{\rm erg\,s^{-1}}}$	$r_{\rm bub}$ (kpc)	$\frac{E_{\rm gas}}{E_{\rm input}}$	$\dot{M}_{\rm SMBH}$ ($\rm M_\odot\ yr^{-1}$)	$\dot{M}_{\rm out}$ ($\rm M_\odot\ yr^{-1}$)
NoAGN	None	0	0	–	130	0
vp-L1	Virtual particle	1	0	0.01	750	40
vp-L2	Virtual particle	2	0.2	0.01	550	200
vp-L5	Virtual particle	5	0.5	0.3	8	1300
tk-L1	Thermal	1	0.1	0.01	800	15
tk-L2	Thermal	2	0.2	<0	900	20
tk-L5	Thermal	5	0.3	0.05	0	180
vpc-L1	Virtual particle biconical	1	0.25	0.01	450	130
vpc-L2	Virtual particle biconical	2	0.35	0.04	150	470
vpc-L5	Virtual particle biconical	5	0.75	0.85	20	1900
tkc-L1	Thermal biconical	1	0.2	0.02	650	90
tkc-L2	Thermal biconical	2	0.35	0.035	400	220
tkc-L5	Thermal biconical	5	0.6	0.3	170	750

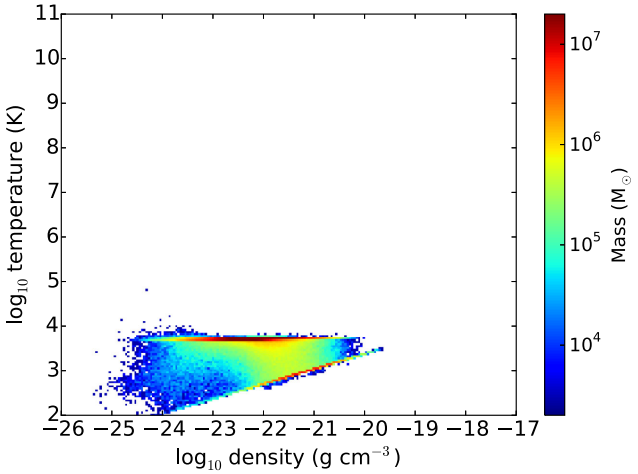

Figure 1. Gas phase diagram just before the AGN switches on. Colour indicates relative density of particles in particular regions of the diagram, with dark blue being lowest and dark red being highest.

3.2 Morphology – spherically symmetric feedback

Fig. 2 shows the density maps of the three virtual particle simulations at $t = 1.5$ Myr, i.e. 0.5 Myr after the AGN switches on, showing the *XZ* plane. The plots use a wedge–slice projection, such that only particles with $|y/r| < 0.25$ are plotted, to ensure that both the innermost regions and the outskirts are well sampled. The three plots reveal a clear change in the global effect of feedback. In the vp-L1 model, feedback is not strong enough to prevent inflow or even to produce significant bubbles; there is only one small cavity in the negative-*X* direction. Simulation vp-L2 shows noticeable outflow bubbles, but simultaneously there exists gas very close to the SMBH, in fact accreting upon the SMBH particle. Most of the feedback energy leaks out in the directions of low density, producing these large bubbles, while the remaining momentum push is too weak to shut off accretion of dense gas. Finally, in vp-L5, we see that feedback is powerful enough to blow away almost all the material, except for a couple of very dense filaments; these remain close to the SMBH, but are also pushed away, albeit slowly.

In Fig. 3, we plot density maps of the analogous tk models, again at $t = 1.5$ Myr. There are significant differences from the vp models. Most noticeably, a well defined almost spherical feedback bubble is present in simulation tk-L5, without any inflow towards the SMBH. On the other hand, the size of the outflow bubble is much smaller in tk-L5 than in vp-L5, since the energy is injected into the gas closest to the SMBH; this gas is dense and therefore cannot be removed as efficiently as the diffuse gas which absorbs most of the input energy in the vp models. It is also interesting to note that the feedback bubble is surrounded by a boundary layer of dense gas, which is not present in the virtual particle simulations. This dense gas cools down very rapidly, so most of the feedback energy is radiated away rather than used to drive bubble expansion.

The major difference between the two models arises because in the thermal feedback simulation, all of the feedback energy is always injected into gas that is closest to the SMBH, typically within the central <200 pc, although the precise radius depends on AGN luminosity and the size of the forming bubble. In the virtual particle simulations, on the other hand, feedback evacuates cavities which allow the virtual particles to stream to large distances of the order of 500–700 pc in the highest luminosity simulation. We now present the effects of changing feedback geometry to conical, which ensures that there is always a channel – the mid-plane of the gas distribution – through which gas can reach the SMBH, and similarly that there is a channel perpendicular to the first through which feedback can be injected at distances comparable to those in the spherical virtual particle model.

3.3 Morphology – conical feedback

Fig. 4 shows the gas density in the three conical virtual particle models, vpc-L1 (left), vpc-L2 (middle) and vpc-L5 (right). Even the lowest luminosity simulation produces a modest outflow, with cavities in the top half and third quadrant of the plot, where the gas was least dense at the time the AGN switched on. The outflow is somewhat conical, but variations in gas density prevent it from acquiring a well-defined shape. In the highest luminosity model, the feedback bubbles are rather large, touching the edges of the initial gas distribution, but gas close to the mid-plane has not been blown away, allowing filamentary inflow to continue. It is worth noting

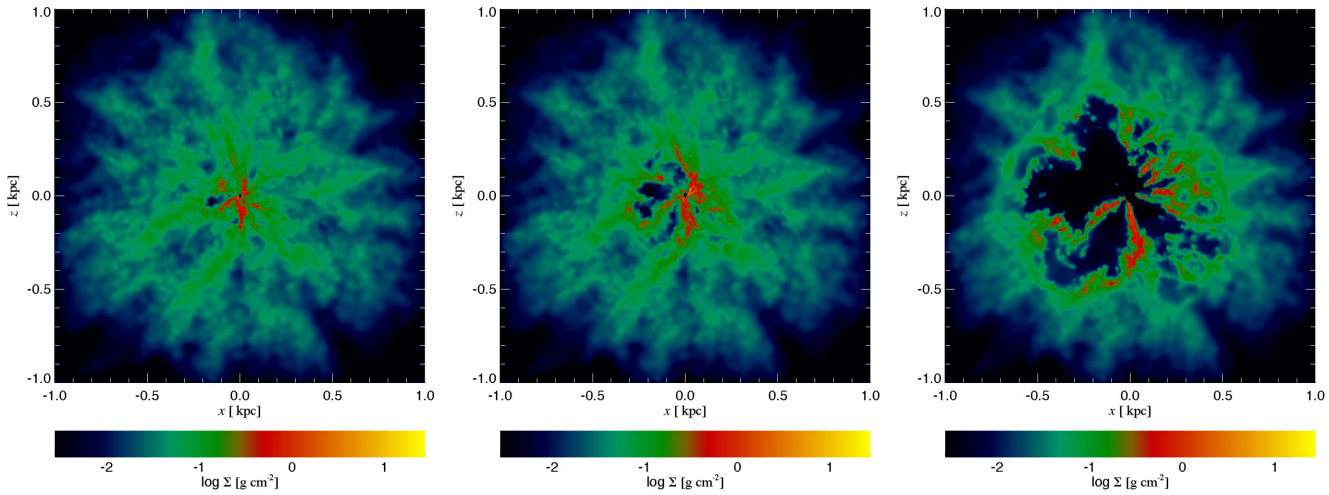

Figure 2. Gas density map in the three virtual particle simulations at $t = 1.5$ Myr: vp-L1 on the left, vp-L2 in the middle, vp-L5 on the right.

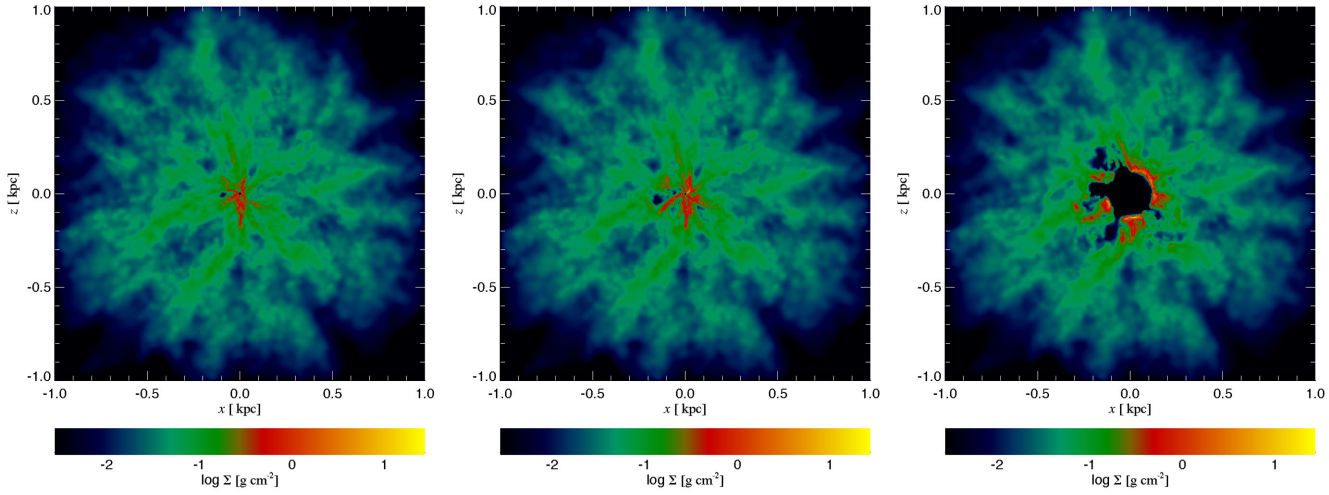

Figure 3. Gas density map in the three thermal models at $t = 1.5$ Myr: tk-L1 on the left, tk-L2 in the middle, tk-L5 on the right.

that the outflow is wider than the opening angle of the cone within which the virtual particles are emitted. This happens because the low-density cavities are overpressurized and expand both vertically and laterally.

Fig. 5 shows the analogous snapshots of the tkc simulations tkc-L1 (left), tkc-L2 (middle) and tkc-L5 (right). Broadly speaking, the simulations evolve similarly to the vpc models; there are two cavities forming in opposite directions and expanding, with material falling in along the equatorial plane. Overall, the differences are much smaller than between the tk and vp models presented above. This happens because with the non-spherical injection of feedback, a channel appears along the equatorial plane which allows inflow and outflow to coexist. Therefore, dense gas no longer accumulates at the edge of a well-defined outflow bubble, but is brought to the mid-plane by the same processes that act in the vpc models. A similar structure of dense inflow along the mid-plane and diffuse outflow in the polar direction develops, with some irregularities due to the turbulent gas density distribution. In the L1 and L2 simulations, both tkc and vpc models produce similarly sized bubbles, while the brightest AGN produces a significantly larger bubble in the vpc simulation. This last size difference is exacerbated by the fact that the bubble reaches the edge of the initial gas distribution in the vpc simulation, and its expansion accelerates. At earlier times, the difference in size between tkc-L5 and vpc-L5 bubbles is much less pronounced.

Despite the morphological differences and similarities, we are more interested in the effect that AGN feedback would have upon the evolution of the host galaxy. Therefore, we now consider several integrated parameters of the system and their time evolution.

3.4 Energetics

One of the most important effects that AGN feedback has upon its host is the energy injection, which leads to gas heating and expulsion. The heated gas then cools down and forms structures including clumps and filaments, as seen in the morphology plots. In order to better understand the difference between thermal and virtual particle feedback prescriptions, we show the phase diagrams of the four L2 simulations in Fig. 6 and correspondingly for the L5 simulations in Fig. 7. In these plots, colour represents the density of particles in the particular parts of the plot, with blue being lowest and red being highest. Dashed lines indicate the bremsstrahlung cooling times.

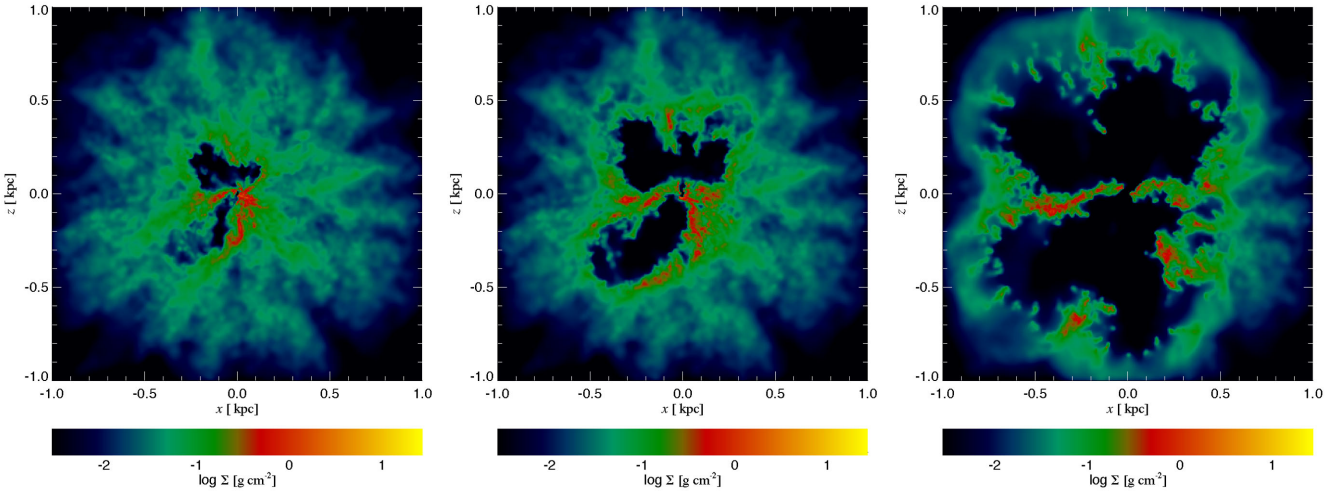

Figure 4. Gas density map in the three conical virtual particle simulations at $t = 1.5$ Myr: vpc-L1 on the left, vpc-L2 in the middle, vpc-L5 on the right.

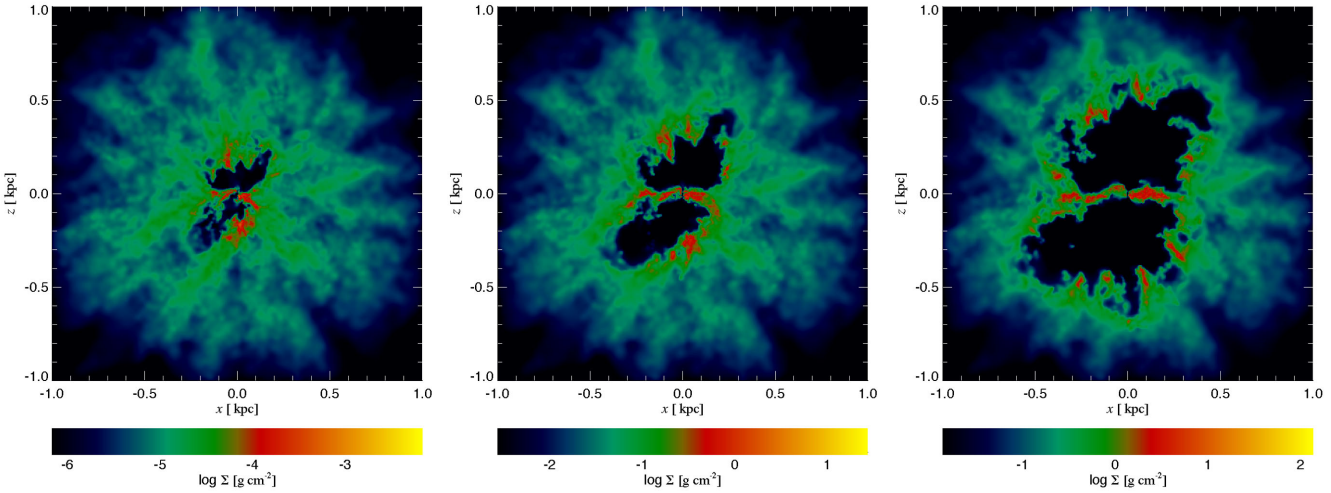

Figure 5. Gas density map in the three conical thermal feedback simulations at $t = 1.5$ Myr: vpc-L1 on the left, vpc-L2 in the middle, vpc-L5 on the right.

A clear difference can be seen between the tk-L2 and vp-L2 models (Fig. 6, top row). Thermal feedback creates slightly more dense gas, which cools down quickly to the two horizontal branches of the equilibrium temperature curve, between 10^4 and 10^5 K. Meanwhile, virtual particle feedback acts upon diffuse gas and heats it up to 10^6–10^8 K. This gas has long cooling times, $t_c > 10^5$ yr and therefore stays hot and flows outwards. Thus, the virtual particle feedback prescription allows the gas to retain a larger fraction of the AGN input energy than the thermal prescription. Such difference is much less pronounced in the conical feedback runs (bottom row), leading to much more similar morphology.

The difference between the tk-L5 and vp-L5 models is even more pronounced (Fig. 7, top row), as the thermal feedback compresses gas close to the SMBH into a very dense shell ($T \simeq 10^4$ K, $\rho > 10^{-19}$ g cm^{-3}). Meanwhile, the virtual particle feedback creates a large population of gas with $T > 10^7$ K, which expands rapidly outwards. Once again, the conical feedback simulations (bottom row) are much more similar to each other, with large amounts of hot expanding gas and much less extremely dense material.

These differences in energy retention are clearly visible when the total gas energy is considered. In Fig. 8, we show the change of total particle energy compared with input energy as a function of time:

$$f_e(t) \equiv \frac{E_{\rm gas}(t) - E_{\rm gas}(1{\rm Myr})}{0.05 L_{\rm AGN}(t - 1{\rm Myr})}; \quad (3)$$

here, the gas energy $E_{\rm gas}$ includes gravitational potential, thermal and kinetic energy. We do not plot the results of the L1 simulations, because they are qualitatively very similar to those of L2, shown in the top panel. The L5 models are in the bottom panel. Virtual particle simulation results are shown in solid lines (black for spherical, blue for conical virtual particle emission), while the thermal feedback simulations are shown in dashed lines (red for spherical, green for conical feedback injection).

In both cases, the conical feedback simulations lose less energy to cooling than spherically symmetric ones. This happens because with conical feedback, dense gas is pushed towards the mid-plane and the heated gas is mostly diffuse, therefore has a low cooling rate (the presence of hot diffuse gas is also seen in the phase plots above). In the L2 models, this low cooling rate is still high enough to make the gas lose most of the injected energy, leaving only a few per cent as the internal energy. However, this is still a factor few better retention than the spherically symmetric model in the virtual particle case;

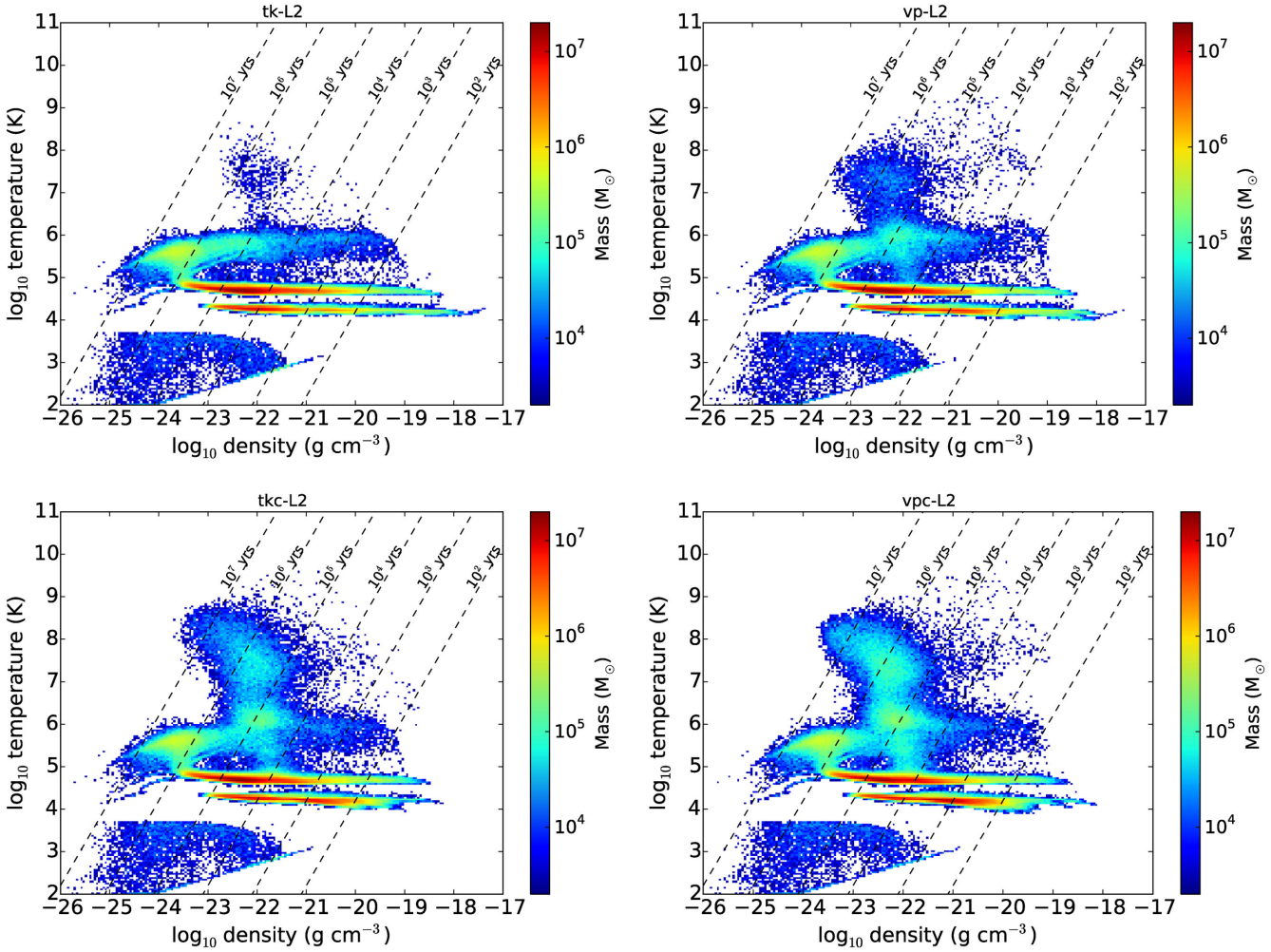

Figure 6. Particle density–temperature plots at t = 1.5 Myr in the four L2 simulations: tk-L2 in the top left, tkc-L2 in the top right, vp-L2 in the bottom left and vpc-L2 in the bottom right. Dashed lines show the expected bremsstrahlung cooling time of the gas and colours indicate relative point density, with red highest and dark blue lowest.

the spherically symmetric thermal feedback model has gas energy decreasing to values even lower than those at $t = 1$ Myr, as gas falls deeper into the potential well. It is worth noting that in the tkc-L2 and vpc-L2 simulations, gas retains very similar amounts of input energy. In the L5 simulations, the virtual particle conical feedback model is essentially purely adiabatic, losing only 10–20 per cent of the input energy by 2 Myr; the thermal conical feedback model loses a much larger fraction of its energy, since it does not create such a large bubble. Even so, the difference between spherical and conical feedback models is significant: energy retention improves by a factor of 5 or more in the thermal model.

Even though the high-luminosity thermal feedback simulation retains significantly less energy than its virtual particle counterpart, the similarity in the L2 models is encouraging. Below we show that similar trends exist in other integrated quantities.

3.5 Inflow and outflow rates

Another particularly important aspect of the co-evolution of SMBHs and their galaxies is the AGN duty cycle, i.e. the frequency and duration of AGN activity episodes. In a realistic system, one might expect AGN feeding and feedback to occur simultaneously, at least up to some critical AGN luminosity. Within the AGN wind feedback model, this happens because most of the AGN wind energy is carried away by low-density gas, allowing dense clouds to fall in towards the SMBH. Although our simulations do not resolve the scales of SMBH feeding, we nevertheless can investigate the ability of various feedback prescriptions to reproduce simultaneous inflows and outflows. For this, we plot the radial profiles of gas inflow and outflow rates in the L2 and L5 simulations in Figs 9 and 10, respectively. The plots are made at three times for each simulation, 0.25, 0.5 and 0.75 Myr after the AGN switches on. The inflow rate is defined as

$$\dot{M}_{\rm in} = m_{\rm SPH} \sum_{{\rm i}\in(v_{\rm r}<-\frac{\sigma}{2})} \frac{|v_{\rm r,i}|}{\Delta R} = 4\pi R^2 v_{\rm r,in} \langle \rho_{\rm in} \rangle, \quad (4)$$

where $\Delta R = 0.1$ kpc is the thickness of the radial bin and the sum goes over all particles with radial velocity directed inward and higher in magnitude than half the background velocity dispersion. The second equality shows that the inflow rate can be expressed via the mean inflowing gas density $\langle \rho \rangle$ and does not depend on the choice of ΔR so long as the bin is thick enough to sample a large number of particles. We neglect particles with small negative velocities because those are dominated by turbulent motions rather than inflow or outflow. The outflow rate is defined in the same way,

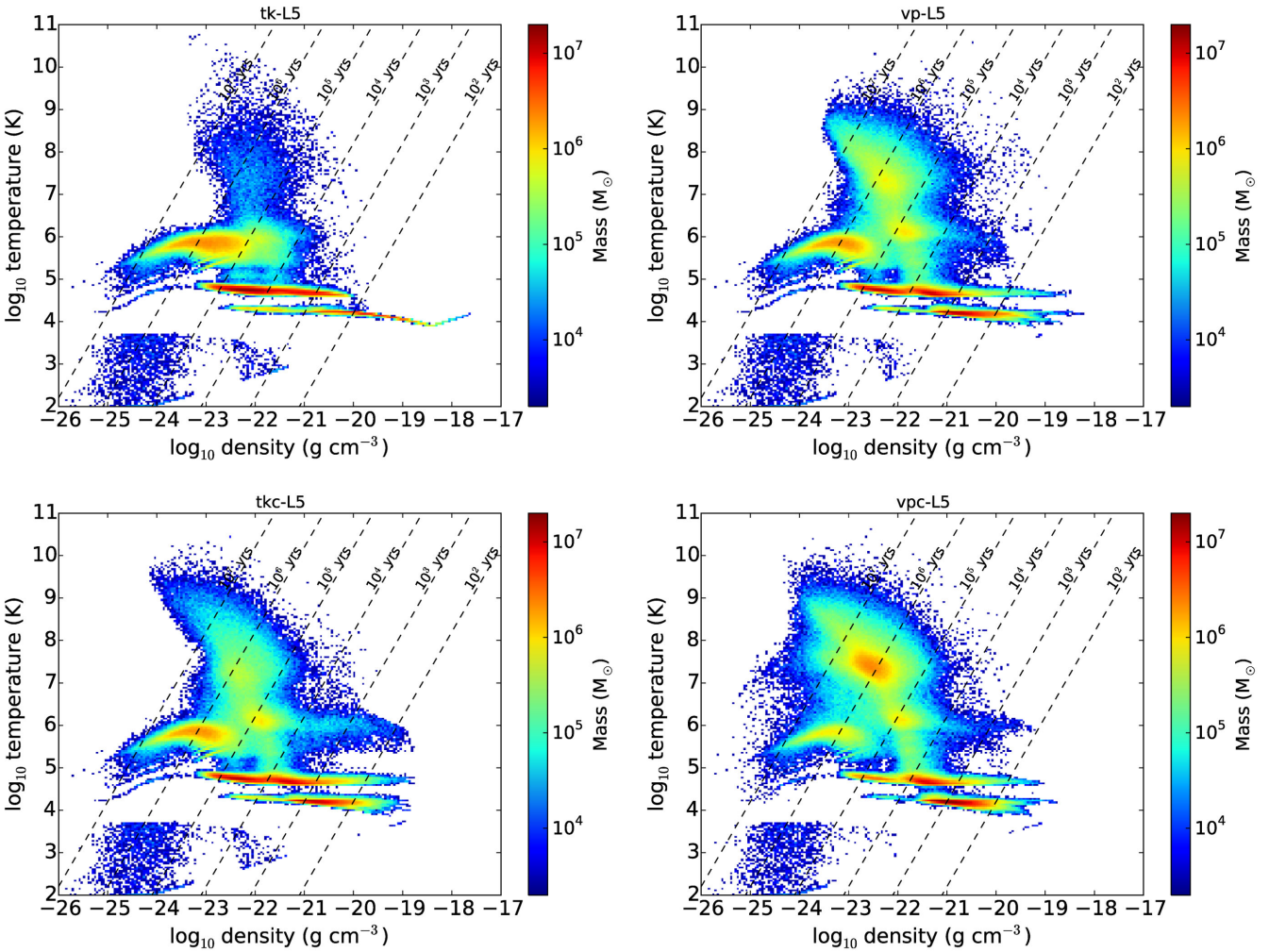

Figure 7. Same as Fig. 6, but for the four L5 simulations.

but the sum is made over all particles with radial velocities greater than half σ.

The four L2 models all generally have stronger inflows than outflows. This is expected, since the AGN luminosity is not large enough to drive away all the gas by momentum push alone. However, clear differences are visible among the models, with tk-L2 having essentially zero outflow, vp-L2 having outflow rates 10–20 times lower than inflow, tkc-L2 having outflow rates only 2–3 times smaller, especially in the region $r = 0.2$–0.5 kpc, and finally vpc-L2 having inflow and outflow rates of comparable magnitude. We see that the qualitative difference present between the tk-L2 and vp-L2 models disappears when feedback is injected conically, even though a notable quantitative difference remains. It is also worth noting that the morphology of all four L2 models appears very similar in the outer regions, since the outflows are never fast enough to extend beyond $\sim$0.5 kpc in 1 Myr.

The L5 models display much greater differences among themselves. The tk-L5 simulation produces very little outflow and a strong inflow, rather similar to its lower luminosity counterpart. However, the inflow proceeds only to $r \simeq 0.1$ kpc and stalls there. In the other three simulations, outflows dominate, initially in the inner regions (black lines), but later throughout the simulation volume. The two conical feedback simulations have qualitatively very similar radial profiles of both inflow and outflow, echoing the similarity in their morphologies (Figs 4 and 5). It is important to note that even though the outflow is very powerful, the inflow rate in the central $\sim$0.15 kpc is similar to the outflow rate, showing the SMBH may be fed even while producing such a massive outflow.

We also plot the time evolution of the rate of gas particle accretion by the SMBH particle (Fig. 11) and the total rate of gas outflow, approximated as

$$\dot{M}_{\rm out} \simeq m_{\rm SPH} \sum_{{\rm i}\in(v_{\rm r}>\frac{\sigma}{2})} \frac{v_{\rm r,i}}{R_{\rm i}} \qquad (5)$$

(Fig. 12). The line colours are as in Fig. 8. In all models, there is no accretion for the first 0.2 Myr of AGN activity, because the gas is falling towards the significantly reduced accretion radius of the SMBH particle.

Here, the two spherically symmetric models are more similar than when the energy retention is considered. However, there is an important qualitative difference. In the tk-L5 model, thermal feedback is able to shut off accretion entirely, by keeping the gas at the edge of a well-defined bubble (see Fig. 3, right-hand panel). On the other hand, the virtual particle model, while producing very large outflow bubbles, also allows some gas to fall on to the SMBH particle. The accretion rate is comparatively small, hardly exceeding $20\,{\rm M}_\odot\ {\rm yr}^{-1}$, but the possibility of accretion is significant. In the

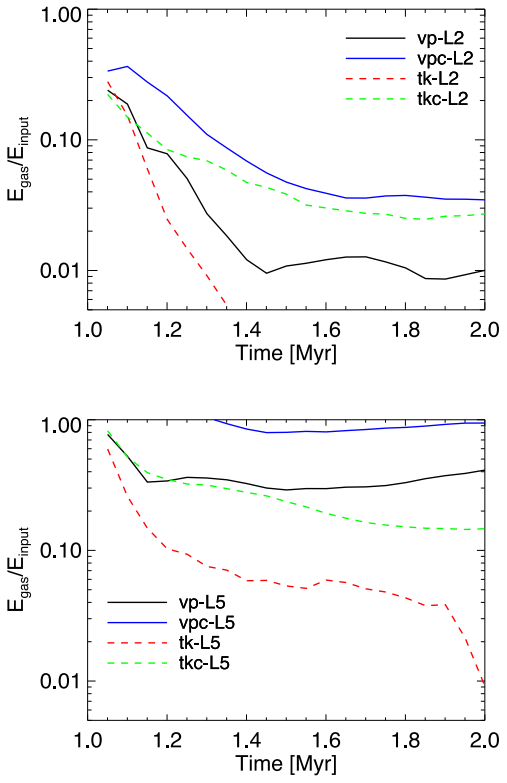

Figure 8. Time evolution of the ratio between AGN input energy and change in total gas energy in the four L5 simulations (top) and four L2 simulations (bottom). Simulations vp-L2 and vp-L5 shown in black solid line, vpc-L2 and vpc-L5 – blue solid, tk-L2 and tk-L5 – red dashed, tkc-L2 and tkc-L5 – green dashed.

L2 models, the situation is reversed: thermal feedback suppresses accretion for ∼0.4 Myr, but then the outflow bubble collapses and accretion rate rises rapidly to $>1000\,M_\odot\ yr^{-1}$. Meanwhile, the vp-L2 models has a steadily rising accretion rate, without such sudden changes.

Both high-luminosity conical feedback models, unsurprisingly, allow far more accretion on to the SMBH. Simulation vpc-L5 is more efficient at pushing gas away than the tkc-L5 simulation, therefore the accretion rate is significantly lower, only rising to a peak of $\sim 45\,M_\odot\ yr^{-1}$. The thermal feedback model, on the other hand, allows accretion at rates approaching $200\,M_\odot\ yr^{-1}$ at $t = 1.25$–1.6 Myr.

In the low-luminosity models, conical feedback actually decreases the gas inflow rate by a factor of few. This happens because in these models, outflow bubbles form and prevent accretion in some directions, channelling accreting material towards the mid-plane. The tkc-L2 simulation has a higher accretion rate at first, since it is initially more efficient in compressing the gas towards the mid-plane, but from $t = 1.7$ Myr onwards, the two accretion rates become very similar.

The difference among the gas outflow rates (Fig. 12) is far more striking. The spherical thermal feedback model is incapable of driving a significant outflow in either low- or high-luminosity models, as most of the AGN input energy is radiated away, and the gas is kept in a dense, but small and hardly expanding, shell. The spherical virtual particle simulation produces an outflow with at least several times higher mass flow rate, and in the higher luminosity case, the outflow rate approaches that of the conical simulations by $t = 2$ Myr. This happens because of the complex morphology present in the virtual particle simulation, with outflowing gas being diffuse, and hence reaching very high velocities.

The conical feedback models produce significant outflows, essentially because the dense gas is channelled away and diffuse gas can

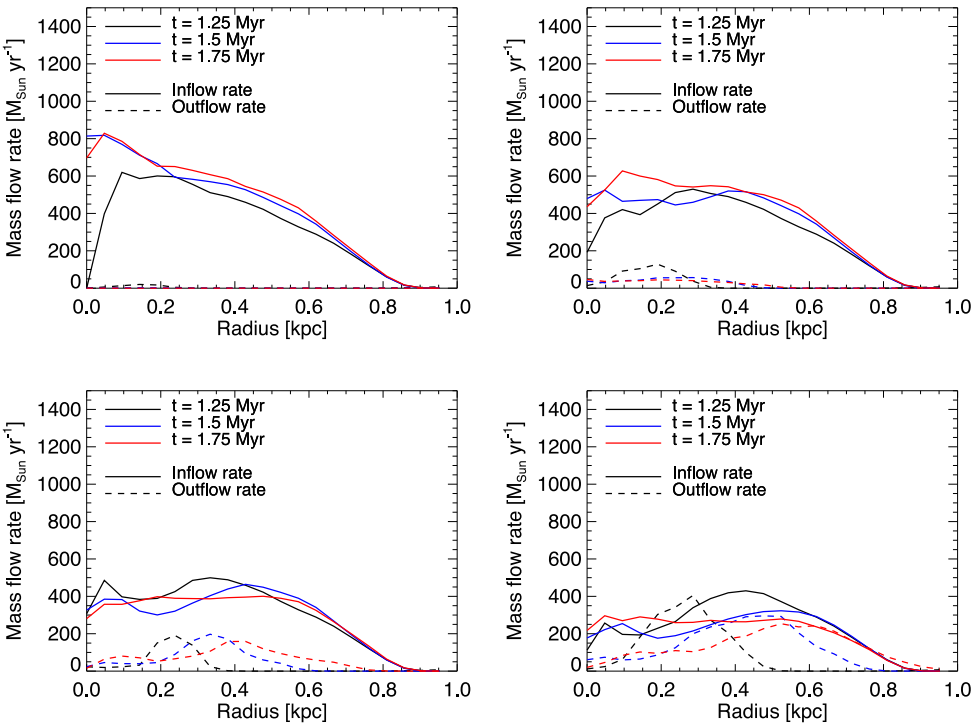

Figure 9. Radial profiles of gas outflow (dashed lines) and inflow (solid lines) rates for three different times in the four L2 models: tk-L2 on the top left, vp-L2 on the top right, tkc-L2 on the bottom left and vpc-L2 on the bottom right.

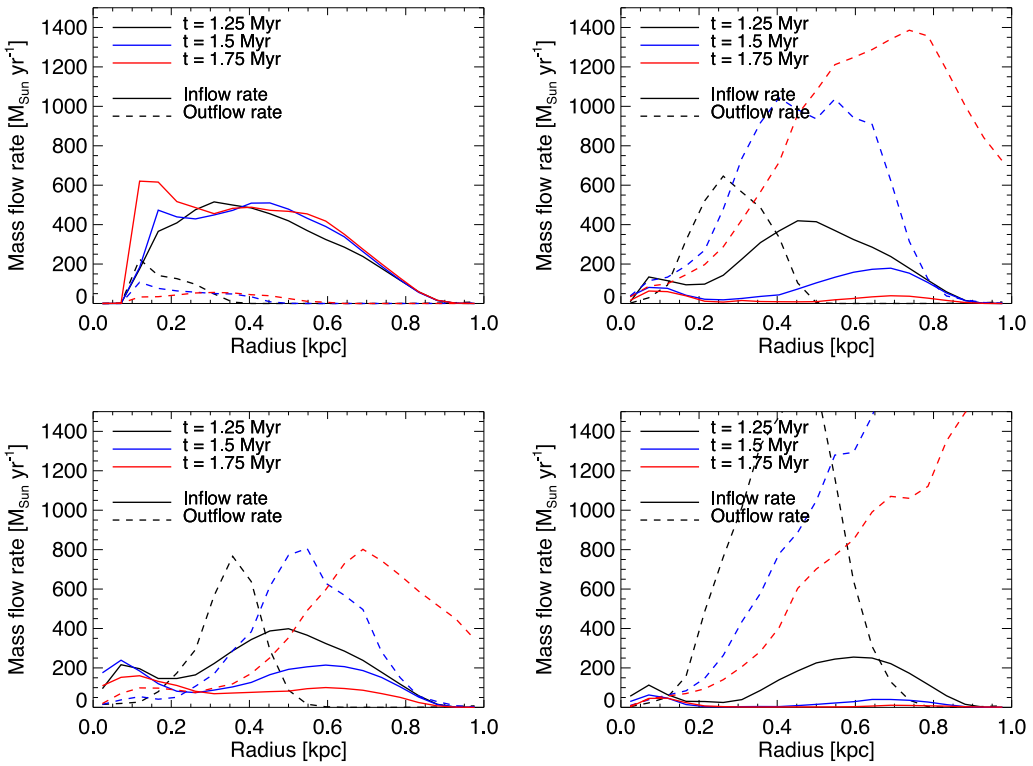

Figure 10. Same as Fig. 9, but for the L5 simulations: tk-L5 on the top left, vp-L5 on the top right, tkc-L5 on the bottom left and vpc-L5 on the bottom right.

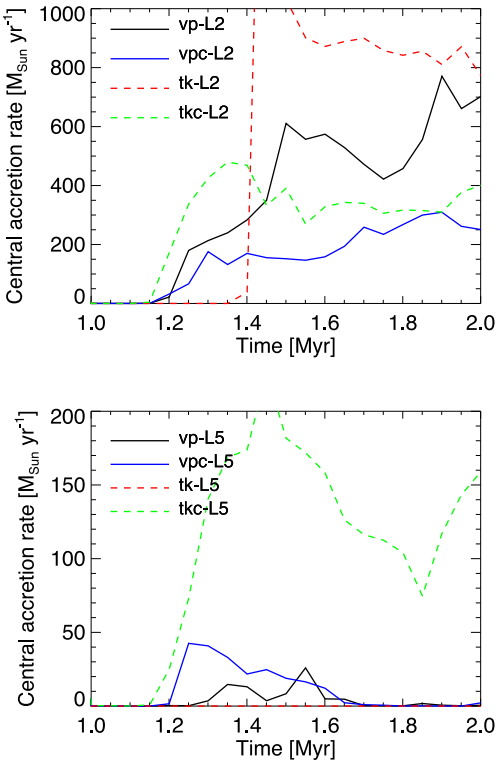

Figure 11. SMBH particle accretion rate as function of time during the AGN activity episode in the four L2 models (top) and L5 models (bottom). Colours and line styles as in Fig. 8.

be accelerated to high velocities. The mass outflow rates approach 2000 $M_\odot$ yr^{-1} in the L5 models. It is interesting that the collimation of feedback into a cone actually increases the outflow rate in the virtual particle simulations, most likely because conical feedback produces more spatially distinct regions of inflow and outflow, so there is less mixing between inflowing and outflowing gas, which would lead to lower outflow rates. The thermal feedback model produces a significantly weaker outflow than the virtual particle model in the conical case as well, but the ratio between outflow rates is much smaller than for the spherical feedback injection simulations.

3.6 Density structure

In Fig. 13, we plot information regarding the evolution of gas density distribution during the AGN activity episode. More precisely, we plot the values of the 10th, 25th, 75th and 90th percentile of the gas density distribution, in order to evaluate how the different phases of gas (diffuse, medium and dense) behave during the AGN activity episode. The line colours and styles are the same as in previous time evolution figures.

We see that the diffuse gas evolves almost identically for the whole AGN activity episode in the L2 models and for the first ∼0.5 Myr in the L5 models, mostly because most of this gas is far away from the SMBH and is not affected by the AGN outflow at first. None of the L2 models produces a bubble extending to the outskirts of the gas sphere, so there is little evolution of the diffuse gas in this model throughout the time period considered; the same is true for the tk-L5 model. In the other three models, diffuse gas starts to become even more diffuse as the outflow bubble moves past it and disperses the gas in a larger volume.

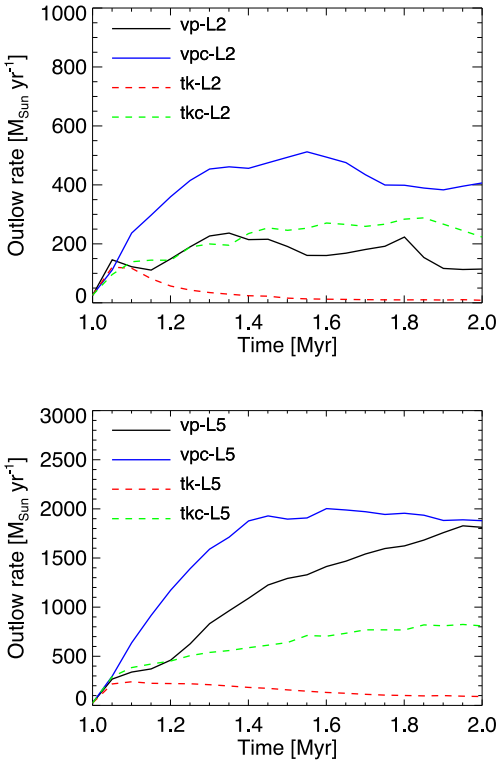

Figure 12. Gas outflow rate as function of time during the AGN activity episode in the four L2 models (top) and L5 models (bottom). Colours and line styles as in Fig. 8.

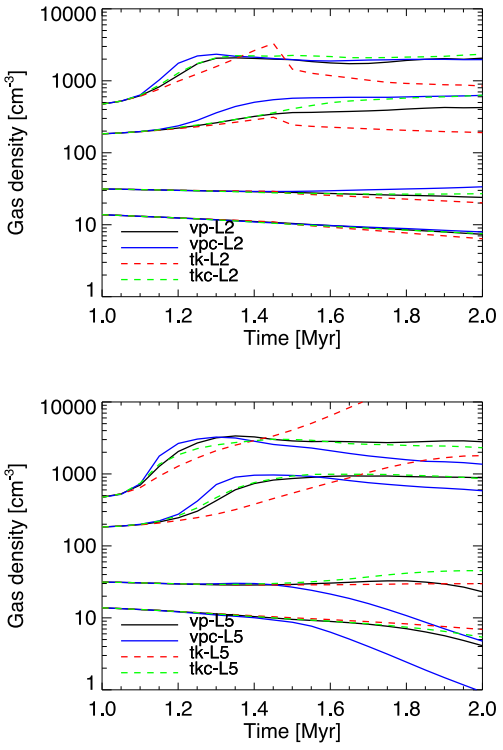

Figure 13. 10th, 25th, 75th and 90th percentiles of the gas particle density distribution as function of time during the AGN activity episode in the four L2 models (top) and L5 models (bottom). Colours and line styles as in Fig. 8.

The dense gas becomes progressively more dense, but with certain differences among the simulations. The virtual particle models compress the dense gas by ∼5–10 times in the period between ∼1.05–1.3 Myr, corresponding to the formation of a complex inflow–outflow structure with many dense clumps and filaments. The tkc-L5 model shows a similar behaviour for the densest gas, although the compression takes a slightly longer time. Once this structure is in place, however, density does not increase further, as the densest material either turns into sink particles or is accreted on to the SMBH. The tk-L5 model, on the other hand, shows essentially unrestricted density growth, because here, the densest gas is also the warmest, because it receives all the AGN energy input, and therefore cannot fragment. The tk-L2 model behaves in the same fashion initially, but later the dense gas collapses on to the SMBH and is accreted, resulting in a drop in the densest gas density values.

4 DISCUSSION

4.1 Summary of results

Our suite of 13 simulations allowed us to explore the effect that the subgrid AGN feedback prescription has upon the evolution of a turbulent gas sphere. Our main results are as follows.

(i) Spherically symmetric thermal AGN feedback is unable to reproduce the complex structures found in virtual particle models. The reason is that the thermal feedback prescription injects energy only into the surrounding gas, creating a well-defined bubble around the SMBH.

(ii) The virtual particle prescription allows for simultaneous gas inflow and outflow, as well as formation of dense gas filaments and clumps, which are not found in the thermal feedback case.

(iii) Replacing both prescriptions with biconical versions results in a marked improvement in their agreement. In particular, the morphologies of the two models then become very similar, with clear outflow bubbles coexisting with inflow along the equatorial plane.

(iv) The conical feedback models are qualitatively similar to the corresponding spherical virtual particle simulations, but quantitatively very different from both spherical models: the outflow bubbles produced by conical feedback are generally larger, the outflow rates higher and much more of the AGN input energy is retained by the gas.

(v) The fraction of AGN input energy retained in the gas is very low in the spherically symmetric thermal feedback simulation, even at high AGN luminosity, but increases to ∼20–30 per cent in the conical high-luminosity one. In the virtual particle models, the energy retention fraction increases to an ever higher value of 70–80 per cent.

(vi) Spherically symmetric thermal feedback either does not allow any accretion on to the SMBH, or allows most of the gas to fall in. It also produces only a weak outflow. Virtual particle and conical models produce both significant inflow and outflow at the same time.

Although the setup of our simulations is strongly idealized, the results have several implications for the understanding of AGN activity and its effects upon the host galaxy. We discuss those implications below.

4.2 Major issues with thermal feedback models

As mentioned in the Introduction and Model sections, the commonly used thermal–kinetic AGN feedback models suffer from a number

of drawbacks. The most important drawback is the assumed spherical symmetry, i.e. energy injection into gas close to the SMBH. If it happens that there is gas only to one side of the SMBH, all the energy will be injected into this gas, rather than spread around symmetrically. This creates a paradoxical situation where assumed spherical symmetry results in energy injection which is often very far from symmetric.

The problem with this energy injection in generating outflows lies in the fact that once any parcel of gas escapes far from the SMBH, it is no longer affected by feedback. Therefore, as far as most gas particles in the simulation are concerned, feedback is very intermittent, and this leads to much weaker outflows than would be possible if feedback acted upon a gas parcel for a prolonged period of time. A small amount of gas does experience this prolonged feedback, however, it gets squashed between AGN feedback on one side and inflowing gas on the other. Gas density therefore increases, cooling becomes more efficient and progressively more of the feedback energy is lost to radiation rather than used to drive the outflow. Therefore, the resulting AGN outflow is much weaker than it would otherwise and more energy is required to remove the gas from the host galaxy than it would be if these multiphase effects were treated properly.

These issues do not necessarily impact the ability of cosmological simulations to reproduce the mass functions and growth histories of present-day galaxies and SMBHs, even though the latter requires appropriate tuning of feedback parameters (Crain et al. 2015; Schaye et al. 2015). AGN accretion and feedback self-regulate in these simulations, so that a less efficient AGN feedback allows more accretion which in turn increases the outflow rate, having a negligible effect upon the long-term evolution of the total stellar mass in the galaxy (Sijacki et al. 2007; Schaye et al. 2010, 2015). However, as such models, as well as models of isolated galaxies, become more detailed, they start reproducing other, smaller scale, processes and structures, such as the phase structure of the gas, the spatially resolved history of star formation, the duration of AGN episodes, and so on. All of these, and many other, properties of the galaxy are affected by the details of how AGN feedback interacts with the ISM, and therefore understanding the limitations imposed by the numerical feedback scheme is of paramount importance when interpreting the results of these models.

Ideally, one would like to minimize the limitations of the numerical method. Our proposed scheme of injecting feedback energy into a cone alleviates the two biggest issues of thermal feedback prescriptions described above. While it does not really resolve the interaction of the AGN outflow with the multiphase gas, it creates a possibility for the gas to remain in two phases (cold dense inflowing and hot diffuse outflowing) while interacting with the outflow. Dense gas is quickly channelled to the bottom of the effective potential well, i.e. to the regions where feedback does not counteract gravity. Once there, dense gas can form filaments which feed the SMBH or fragment into self-gravitating clumps. Meanwhile, diffuse gas gets heated and pushed by the feedback energy injection and forms a massive outflow which cools slowly due to low gas density. This results in an adiabatic outflow, consistent with the analytical predictions of the wind feedback model.

4.3 Possible improvements to cosmological simulations

Given that a conical thermal feedback prescription is capable of resolving a lot of the complexity of simultaneous inflows and outflows with little extra computational cost, we suggest that it may be interesting to explore its effects in cosmological simulations, which self-consistently track the growth and energy release from AGN over long time-scales. This would allow one to constrain the AGN growth scenarios, the M–σ relation, the effects of AGN outflows upon galaxies and clusters, the triggering of star formation, as well as the history of SMBH growth, with better precision than is currently available (Schaye et al. 2015). One particularly interesting consequence might be that the presence of simultaneous inflows and outflows around SMBH change the qualitative behaviour of AGN self-regulation (see Section 4.4 below).

A few important aspects have to be considered when implementing this scheme into cosmological simulations. The first is numerical resolution, which is typically much worse in cosmological simulations than it is in the simulations presented here. In a previous paper (Bourne et al. 2015), we investigated the importance of resolution upon the efficiency of feedback and found that low-resolution simulations produce feedback that is much more negative. This happens in part because those simulations are unable to resolve the complex structures developing in the turbulent ISM. With a conical feedback prescription, it should be easier to resolve those structures, since the cavities and filaments are larger (compare the right-hand panels in Figs 2 and 4). However, we may still expect a weaker overall effect of AGN feedback due to the fact that the gas density contrast is not resolved as well, leading to overcooling of the hot gas in the bubbles.

Another aspect is defining the appropriate direction of the cone's axis. We suggest that this axis should coincide with the axis of rotation of the SMBH particle. Rotation can be tracked by tracking the angular momentum magnitude and direction of the infalling gas, and the plane of the accretion disc should be perpendicular to this axis of rotation. Since the AGN outflow originates in the disc, it is reasonable to assume that it goes in the polar direction (Feldmeier & Shlosman 1999). The opening angle of the wind cone is a free parameter, which might be constrained by more detailed models, or investigated empirically. However, such an investigation is beyond the scope of this paper.

Finally, cosmological simulations contain galaxies which have varied structures, including discs, large clumps and cavities created by previous outflows. The interaction of a new outflow with these structures may be much more complex than in our simulations presented above. For example, one directed conical outflow might intercept a dense clump and lose a large fraction of its energy, while another may expand into a pre-existing cavity, having little effect upon the mass budget in its host galaxy. A more thorough investigation of feedback prescriptions in a more realistic galaxy model should be done before implementing them into a cosmological simulation. We intend to perform such tests in a future publication.

4.4 Self-regulation of AGN activity

Our simulations use a fixed AGN luminosity rather than keeping it tied to the central particle accretion rate. Given that the central accretion rates in different simulations can differ by orders of magnitude (see Fig. 11), this may seem as a significant drawback of the numerical setup. However, we feel that simulations addressing just the feedback aspect of AGN activity are still very useful since the models with feedback determined by BH accretion rate employ a number of assumptions about this rate. Given the non-linear accretion-feedback connection, it would be hard to arrive at definite conclusions about the feedback efficiency in these more complex and less constrained simulations. In addition, the actual expected evolution of the system is somewhat more complicated than the accretion rate of the central particle would suggest. Infalling gas

contains some angular momentum, and therefore forms an accretion disc around the SMBH, rather than falling in directly. Given that in the simulations the accretion rate is measured at a radius of 10 pc, most of this accreting gas will take far longer than 1 Myr to reach the SMBH, by which time the activity episode in our test run is over. Additionally, some of this gas will fragment and form a nuclear star cluster rather than feeding the SMBH (Nayakshin 2006), further reducing the impact upon the AGN luminosity. Therefore, our simulations may be seen as an investigation of how a large-scale gas distribution is affected by AGN activity caused by accreting a cloud of pre-determined mass, from $M_{\rm accr} = 2.2 \times 10^6\,{\rm M}_\odot$ (L1 simulations) to $M_{\rm accr} = 1.1 \times 10^7\,{\rm M}_\odot$ (L5 simulations).

In a more realistic simulation, long-term self-regulation of AGN activity becomes important. Here, the temporal evolution of simulations using the thermal–kinetic and virtual particle feedback prescriptions might be very different from one another. When the AGN luminosity increases, simulations using the spherically symmetric thermal–kinetic AGN feedback prescription abruptly change from a situation where no outflow is occurring to one where the outflow completely shuts off AGN accretion. This latter situation may reverse after some time, as the material piles up at the edge of the outflow bubble, and its weight may overcome the force produced by AGN feedback, leading to collapse and resuming of accretion. However, while the bubble holds, there is no accretion. Conversely, while there is accretion, no outflow bubble can exist. This 'all-or-nothing' situation places tight constraints on the regulation of AGN accretion rate. When the AGN is fed at a large enough rate, an outflow forms and shuts off accretion. As the accretion rate drops to zero (with perhaps some delay imposed in the simulation to mimic the draining of the subresolution accretion disc), AGN luminosity also decreases and feedback stops, allowing accretion to resume. We may therefore expect AGN activity to keep switching on and off, with the duration of the 'on' phase comparable to the viscous time-scale of the accretion disc ($t_{\rm on} \sim 10^5$–10^6 yr) and the 'off' phase lasting for as long as it takes for gas to fall back to the SMBH ($t_{\rm off} > 10^6$ yr). These time-scales are comparable to some estimates of the lifetimes of AGN phase (Schawinski et al. 2015), but this is only coincidental, since the processes described here happen due to numerical, rather than physical, reasons.

The virtual particle prescription, as well as both conical prescriptions explored in this paper, allow simultaneous inflow and outflow to coexist. At some point, the larger gas reservoir gets depleted and accretion switches off, leading to a longer period of inactivity than in the case of spherical thermal feedback. This simulation therefore does not manifest an artificial short-time-scale 'flickering' and can be used to investigate the physical reasons of the switching on and off of AGN activity.

On the other hand, some integrated parameters, such as the total mass accreted by the SMBH or expelled from the galaxy, may not differ very much between thermal–kinetic and virtual particle feedback simulations. The reason for this is simply that on long time-scales SMBH accretion tends to self-regulate so that the total energy release into the surrounding medium is just enough to balance gravity (Booth & Schaye 2009). A thermal–kinetic feedback prescription would lead to faster accretion followed by a stronger burst of AGN activity, which leads to a larger feedback bubble and shutting off accretion for a longer time. The virtual particle prescription would result in a more uniform accretion and outflow rate, with neither undergoing such strong changes as in the thermal–kinetic feedback model. As a result, eventually the results of the two simulations might look more similar to each other than might seem from our simulation results. Still, on short time-scales, the morphology and temporal variability of inflow and outflow rates would differ significantly among the simulations.

The possibility of having prolonged periods of AGN activity coincident with SMBH growth via accretion also has an implication for the growth of the very first SMBHs. These black holes (BHs) are known to have masses exceeding $10^9\,{\rm M}_\odot$ by $z = 6$, when the Universe was $<10^9$ yr old (e.g. Wu et al. 2015). If these SMBHs grew from stellar mass progenitors, their growth rate must have been close to the Eddington limit for most of their lives (King & Pringle 2006). The possibility of having rapid gas inflows during the AGN phase suggests that this might be easier than previously thought and eliminates one of the potential drawbacks of this growth mechanism in explaining the large observed masses. We note, however, that it is possible to grow BHs to the required masses at high z even with the typical thermal–kinetic AGN feedback prescription (Di Matteo et al. 2012), at least for seed SMBH masses of $10^5\,{\rm M}_\odot$. Therefore a change in our understanding of accretion and feedback is not necessary to explain the high-z quasars.

4.5 Implications for positive AGN feedback

Thermal feedback simulations, both spherically symmetric and conical, eliminate some of the structure present in turbulent gas. Meanwhile, virtual particle simulations, and to some extent the conical thermal feedback simulations, enhance some of the structures, by enveloping dense gas in hot diffuse bubbles and compressing it more than self-gravity alone would. This leads to formation of more clumps and more efficient star formation within them (Zubovas, Sabulis & Naujalis 2014), resulting in a higher rate of fragmentation and star formation. In other words, AGN activity has a positive feedback upon star formation in the host galaxy.

This effect has been explored in previous numerical works. Nayakshin, Sazonov & Sunyaev (2012) showed that the outflowing material can fragment as it cools down, leading to potentially rapid star formation and stars ejected from host galaxies. Gaibler et al. (2012) explored the interaction of an AGN jet with a clumpy ISM and found that the jet compresses dense gas, prevents adiabatic re-expansion of the clumps, and enhances the SFR of the whole galaxy. There is also tentative observational support that galaxies with more luminous AGN have higher SFRs and efficiencies (e.g. Wang et al. 2010; Wei et al. 2010), although the causal connection is not certain.

We chose not to consider in detail the fragmentation of gas in our simulations, as that is not the main point of this study. Nevertheless, we find qualitatively similar effects, but, importantly, they are much more significant in the virtual particle feedback models, where the multiphase ISM is affected by feedback based on its density. In a more realistic simulation, the effects of AGN outflow, and of the numerical prescription used to track its interaction with the ISM, might significantly affect the fragmentation rate and spatial locations in the galaxy. We suggest that using a more detailed AGN feedback prescription, such as the conical thermal feedback one, would allow investigating this positive feedback in a far more realistic way.

4.6 How realistic is the virtual particle simulation?

One implicit assumption we made so far when analysing the results is that the virtual particle feedback prescription is a good representation of reality. The method certainly has several advantages over the thermal feedback model. It is truly isotropic, i.e. feedback energy is emitted in all directions from the AGN and interacts with

the ISM in all directions independently of the shape of the cavity surrounding the AGN. In addition, the model, by construction, accounts for the different optical depths of gas in different directions, leading to situations where a dense clump can shield the gas behind itself from being blown away.

On the other hand, the model suffers from some shortcomings as well. The interaction cross-section between virtual particles and SPH particles is a free parameter of the model. This means that the depth to which virtual particles penetrate the gas can vary significantly between simulations. As a result, dense gas clumps can sometimes be obliterated unphysically rapidly. Conversely, in other cases, gas might be compressed too strongly where a gentler push would be more realistic and represent the many filaments forming along the contact discontinuity between the AGN wind and the shocked ISM.

Another drawback is that the virtual particles are assumed to always propagate radially out from the AGN. This is unrealistic in cases of uneven density, where a steep density gradient may be present in a direction not parallel to the direction of propagation of the virtual particle. In this case, a realistic interaction would have the virtual particle flying off at an angle to its initial direction, something which the present model does not allow. This drawback may have many subtle effects in how the gas morphology is affected by AGN activity.

Given these drawbacks, we stress that the results of the virtual particle simulations should not be considered as perfect representations of reality. However, given that they reproduce a far more complex morphology of the turbulent ISM and properties of outflows in agreement with observations, we believe that their results represent real galaxies better than those of the spherical thermal feedback models.

5 CONCLUSION

In this paper, we presented a number of simulations of AGN feedback affecting a turbulent gas sphere. The simulations are designed to show the impact of different subgrid recipes of AGN feedback upon the evolution of the whole system. We show that the commonly used spherically symmetric thermal AGN feedback prescription is unable to reproduce the variety of complex structures observed in more detailed models, fails to reproduce the observed rapid massive outflows and in general has a much weaker effect on the host galaxy than predicted by analytical calculations of feedback models.

On the other hand, a relatively simple improvement to the prescription – injecting energy into a cone rather than a sphere – alleviates most of these issues. The outflows become rapid, massive and close to adiabatic, dense structures and inflowing filaments coexist with outflowing gas, and gas fragmentation rates are significantly increased. In particular, even extremely bright AGN are unable to shut off gas accretion completely, allowing the SMBH to continue growing. We suggest that this improvement could be used in cosmological simulations in order to better model the effects that AGN have on their host galaxies and clusters.

ACKNOWLEDGEMENTS

KZ is funded by the Research Council of Lithuania grant no. MIP-062/2013. MAB and SN acknowledge an STFC grant. MAB is funded by an STFC research studentship. We thank Justin Read for the use of SPHS. This research used the DiRAC complexity system, operated by the University of Leicester IT Services, which forms part of the STFC DiRAC HPC Facility (www.dirac.ac.uk). This equipment is funded by BIS National E-Infrastructure capital grant ST/K000373/1 and STFC DiRAC Operations grant ST/K0003259/1. DiRAC is part of the UK National E-Infrastructure.

REFERENCES

Booth C. M., Schaye J., 2009, MNRAS, 398, 53
Bourne M. A., Nayakshin S., Hobbs A., 2014, MNRAS, 441, 3055
Bourne M. A., Zubovas K., Nayakshin S., 2015, MNRAS, 453, 1829
Cicone C. et al., 2014, A&A, 562, A21
Crain R. A. et al., 2015, MNRAS, 450, 1937
Dehnen W., Aly H., 2012, MNRAS, 425, 1068
Di Matteo T., Khandai N., DeGraf C., Feng Y., Croft R. A. C., Lopez J., Springel V., 2012, ApJ, 745, L29
Feldmeier A., Shlosman I., 1999, ApJ, 526, 344
Feruglio C., Maiolino R., Piconcelli E., Menci N., Aussel H., Lamastra A., Fiore F., 2010, A&A, 518, L155
Gaibler V., Khochfar S., Krause M., Silk J., 2012, MNRAS, 425, 438
King A., 2003, ApJ, 596, L27
King A. R., 2010, MNRAS, 402, 1516
King A. R., Pringle J. E., 2006, MNRAS, 373, L90
Mashchenko S., Wadsley J., Couchman H. M. P., 2008, Science, 319, 174
Nardini E. et al., 2015, Science, 347, 860
Nayakshin S., 2006, MNRAS, 372, 143
Nayakshin S., 2014, MNRAS, 437, 2404
Nayakshin S., Zubovas K., 2012, MNRAS, 427, 372
Nayakshin S., Wilkinson M. I., King A., 2009, MNRAS, 398, L54
Nayakshin S., Sazonov S., Sunyaev R., 2012, MNRAS, 419, 1238
Read J. I., Hayfield T., 2012, MNRAS, 422, 3037
Rupke D. S. N., Veilleux S., 2011, ApJ, 729, L27
Sazonov S. Y., Ostriker J. P., Ciotti L., Sunyaev R. A., 2005, MNRAS, 358, 168
Schawinski K., Koss M., Berney S., Sartori L., 2015, MNRAS, 451, 2517
Schaye J. et al., 2010, MNRAS, 402, 1536
Schaye J. et al., 2015, MNRAS, 446, 521
Sijacki D., Springel V., Di Matteo T., Hernquist L., 2007, MNRAS, 380, 877
Silk J., 2005, MNRAS, 364, 1337
Springel V., 2005, MNRAS, 364, 1105
Sturm E. et al., 2011, ApJ, 733, L16
Tombesi F., Cappi M., Reeves J. N., Palumbo G. G. C., Yaqoob T., Braito V., Dadina M., 2010a, A&A, 521, A57
Tombesi F., Sambruna R. M., Reeves J. N., Braito V., Ballo L., Gofford J., Cappi M., Mushotzky R. F., 2010b, ApJ, 719, 700
Wang R. et al., 2010, ApJ, 714, 699
Wei L. H., Vogel S. N., Kannappan S. J., Baker A. J., Stark D. V., Laine S., 2010, ApJ, 725, L62
Wendland H., 1995, Adv. Comput. Math., 4, 389
Wu X.-B. et al., 2015, Nature, 518, 512
Zubovas K., King A., 2012, ApJ, 745, L34
Zubovas K., Nayakshin S., 2014, MNRAS, 440, 2625
Zubovas K., Nayakshin S., Sazonov S., Sunyaev R., 2013, MNRAS, 431, 793
Zubovas K., Sabulis K., Naujalis R., 2014, MNRAS, 442, 2837

This paper has been typeset from a TEX/LATEX file prepared by the author.